Bioconjugate Chemistry

Article

pubs.acs.org/bc

Self-Sensing Porphysomes for Fluorescence-Guided Photothermal Therapy

Kenneth K. Ng,[†,⊥] Misa Takada,[⊥,‡,¶] Cheng C.S. Jin,[†,⊥,§] and Gang Zheng*[,†,⊥,¶,§]

[†]Institute of Biomaterials and Biomedical Engineering, [¶]Department of Medical Biophysics, and [§]Department of Pharmaceutical Sciences, University of Toronto, Toronto, Ontario M5G 1L7, Canada

[⊥]Princess Margaret Cancer Centre and Techna Institute, University Health Network, Toronto, Ontario M5G 1L7, Canada

[‡]Department of Chemistry, Osaka University, Osaka 560-0043, Japan

Supporting Information

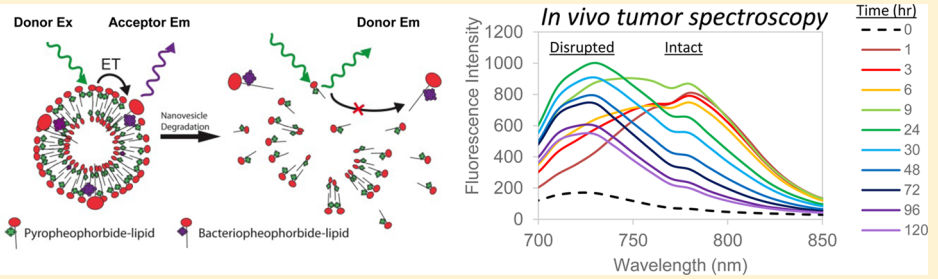

ABSTRACT: Porphysomes are highly quenched unilamellar porphyrin−lipid nanovesicles with structurally dependent photothermal properties. The high packing density of porphyrin molecules in the lipid bilayer enables their application in photothermal therapy, whereas the partial disruption of the porphysome structure over time restores the porphyrin fluorescence and enables the fluorescence-guided photothermal ablation. This conversion is a time-dependent process and cannot be easily followed using existing analytical techniques. Here we present the design of a novel self-sensing porphysome (FRETysomes) capable of fluorescently broadcasting its structural state through Förster resonance energy transfer. By doping in a near-infrared emitting fluorophore, it is possible to divert a small fraction of the absorbed energy toward fluorescence emission which provides information on whether the vesicle is intact or disrupted. Addition of bacteriopheophorbide−lipid into the vesicle bilayer as a fluorescence acceptor (0.5−7.5 mol %) yields a large separation of 100 nm between the absorption and fluorescence bands of the nanoparticle. Furthermore, a progressive increase in FRET efficiency (14.6−72.7%) is observed. Photothermal heating and serum stability in FRETysomes is comparable with the undoped porphysomes. The fluorescence arising from the energy transfer between the donor and acceptor dyes can be clearly visualized *in vivo* through hyperspectral imaging. By calculating the ratio between the acceptor and donor fluorescence, it is possible to determine the structural fate of the nanovesicles. We observe using this technique that tumor accumulation of structurally intact porphyrin−lipid nanovesicles persists at 24 and 48 h postinjection. The development of FRETysomes offers a unique and critical imaging tool for planning porphysome-enabled fluorescence-guided photothermal treatment, which maximizes light-induced thermal toxicity.

INTRODUCTION

Porphysomes are nanovesicles whose main structural component is pyropheophorbide−lipid (pyro-lipid), a semisynthetic derivative of chlorophyll.[1] Porphysomes have previously demonstrated utility as an activatable photosensitizer,[2] photothermal agent,[3] fluorescence probe,[4] MRI contrast agent,[5] and a radionuclide chelator for radioimaging.[6] Due to the high local concentration of the pyro-lipid dye comprising the membrane structure of the nanoparticle, fluorescence and photosensitizing properties of each dye monomer are inhibited through static quenching. Since absorbed light energy is rapidly dissipated through nonradiative pathways such as vibrational relaxation, porphysomes behave as photothermal agents when the nanovesicle structure is intact. Once disruption of the particle occurs, the photothermal conversion efficiency is diminished, while the fluorescence and photosensitizing capabilities of the monomer are restored.

Application of porphysomes for the photothermal treatment of localized solid tumors would benefit from knowledge of the time course of its structural stability. Since the structural stability of porphysomes and its tumor accumulation are time-dependent, there exists an optimal moment which results in the greatest concentration of structurally intact porphysomes in the tumor.

One approach to determining the optimal time of treatment is to track the fluorescence of the porphysomes over time using whole body fluorescence imaging. While fluorescence un-

Received: December 16, 2014
Revised: January 5, 2015
Published: January 7, 2015

DOI: 10.1021/bc500595d
Bioconjugate Chem. 2015, 26, 345−351

quenching provides information on the nanovesicle structure, it is not possible to distinguish between fluorescence arising from tumor accumulation and porphysome unquenching. One way to address this problem is to incorporate a second fluorophore into the porphysome matrix and monitor excitation energy transfer between the dyes through Förster resonance energy transfer (FRET). FRET is a nonradiative energy transfer mechanism that involves a dipole−dipole interaction between two fluorophores separated in space.[7] When a donor and acceptor pair are within the critical distance of interaction, de-excitation of the donor molecule leads to an instantaneous excitation of the acceptor molecule. Typically the distance over which the molecules can interact is between 1 and 10 nm.[8] Due to the spatial sensitivity of the process, FRET has been used to study molecular interactions such as protein−protein interactions[9,10] and lipid dynamics.[11,12] It has also been used as a mechanism for the activation of photosensitizing molecular beacons,[6,13] integrated into nanoplatforms to create long Stokes shift fluorescent probes,[14] and used in the study of nanoparticle stability in polymer micelles,[15,16] lipid nanoparticles,[17] lipid-coated quantum dot micelles,[18] and biomimetic lipoproteins.[19]

Herein, we evaluate the feasibility of integrating a structural sensing functionality into porphysomes through the application of FRET (FRETysomes) (Figure 1). Successful incorporation

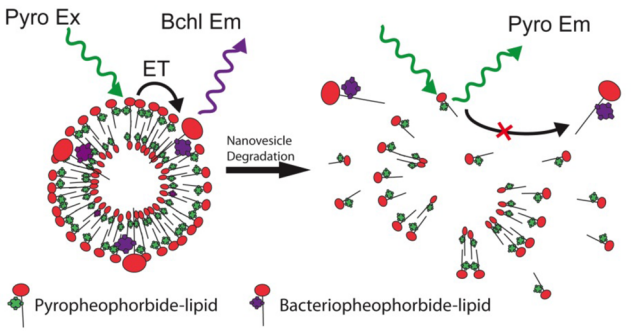

Figure 1. Schematic figure of energy transfer between pyro-lipid donor and bchl-lipid acceptors on the surface of porphysome nanovesicles. Insertion of bchl-lipid into vesicle enables energy transfer from pyro-lipid to bchl-lipid in the intact structure (left). Degradation of the nanovesicle structure will cause separation of dye lipids; thus pyro-lipid emission is recovered and bchl-lipid emission (through energy transfer) is inhibited.

of structural sensing opens up the possibility of studying the *in vivo* structural fate of porphysomes and enables the determination of the optimal time for photothermal treatment.

RESULTS AND DISCUSSION

Selection of Acceptor Fluorophore. Porphysomes are lipid vesicles comprising pyropheophorbide *a*-lipid (pyro-lipid) (55%) combined with cholesterol (40%) and pegylated phospholipid (DSPE-methoxy-PEG$_{2000}$) (5%) to enhance serum stability. Due to the high concentration of pyro-lipid molecules embedded in the vesicle membrane, porphysomes are efficient photothermal transducers. However, the fluorescence from these particles is non-negligible, as fluorescence spectroscopy shows the presence of a weak but present fluorescence peak. Thus, there may be a population of pyro-lipid molecules which can undergo energy transfer. Bacteriopheophorbide *a*-lipid (bchl-lipid), a porphyrin derivative extracted from purple photosynthetic bacteria (*Rhodobacter sphaeroides*) was selected as a fluorescence acceptor since its lowest energy absorbance band overlapped with the emission of pyro-lipid (Supporting Information Figure S1). Furthermore, bchl-lipid has a chemical structure which is similar to that of pyro-lipid and hence should be easily integrated into the nanovesicle membrane.

Effect of Bchl-Lipid Doping on Porphysome Spectral Properties. We first examined the influence of loading various amounts of bchl-lipid incorporated into the pyro-lipid membrane on its spectral properties. Formulations were prepared with bchl-lipid percentages ranging from 0% to 7.5% of the overall fluorescent lipid content (Supporting Information Table S1). Measurement of the particle diameter by dynamic light scattering indicated that neither the *z*-average size nor the polydispersity index changed significantly by increasing the bchl-lipid ratio (Supporting Information Table S1). The absorbance spectra showed an increase in the absorbance peak at 770 nm upon incorporation of bchl-lipid linear increase in bchl-lipid absorbance as its concentration increased in the nanovesicle (Supporting Information Figure S2). This linearity between bchl-lipid loading and its absorbance indicated that bchl-lipid was robustly and accurately doped into the FRETysome lipid membrane.

We next investigated the fluorescence properties of these formulations. To measure the fluorescence emission, both FRETysomes and porphysomes were adjusted to a concentration of 2 μM based on the pyro-lipid concentration. Fluorescence emission spectra were collected by exciting the lowest energy absorption band of pyro-lipid at 633 nm and collecting the emission from 650 to 850 nm. Changes in emission spectra were evident upon increasing the amount of bchl-lipid loaded into porphysomes. Two fluorescence peaks were observed corresponding to pyro-lipid emission (650−700 nm) and bchl-lipid emission (700−850 nm) (Figure 2A). An apparent Stokes shift of ∼100 nm was observed in bchl-lipid doped samples when comparing pyro-lipid absorption and bchl-lipid fluorescence emission (comparing Figure 2A with Supporting Information Figure S2). Increasing bchl-lipid loading led to a decrease in pyro-lipid emission. This quenching can be explained by an increase in energy transfer from pyro-lipid to bchl-lipid which competes with the fluorescence de-excitation pathways in pyro-lipid (Figure 2B). FRET efficiencies calculated from each formulation show a progressive increase in efficiency from 14.6% to 72.7% in the 0.5% bchl-lipid and 7.5% bchl-lipid FRETysome samples, respectively (Supporting Information Table 1).

Increasing the bchl-lipid loading from 0.5% to 5% also led to an increase in bchl-lipid emission (Figure 2B). An increase in loading causes an increase in the population of bchl-lipid molecules in the porphysome membrane. Thus, more acceptor molecules are available to participate in energy transfer. Interestingly, the bchl-lipid emission peak did not increase beyond 5%, despite the fact that pyro-lipid emission continued to decrease. We hypothesize that the plateau in bchl-lipid emission intensity is caused by an increase in aggregation between bchl-lipid molecules, which lowers its fluorescence quantum yield.

To provide further evidence that the bchl-lipid emission peak is caused by energy transfer from pyro-lipid and not through direct excitation of the acceptor dye, two formulations were prepared containing 5% bchl-lipid embedded in porphysomes or in a liposome prepared from 1-palmitoyl-2-oleoyl-*sn*-glycero-3-phosphocholine (POPC). Samples diluted to the same

DOI: 10.1021/bc500595d
Bioconjugate Chem. 2015, 26, 345−351

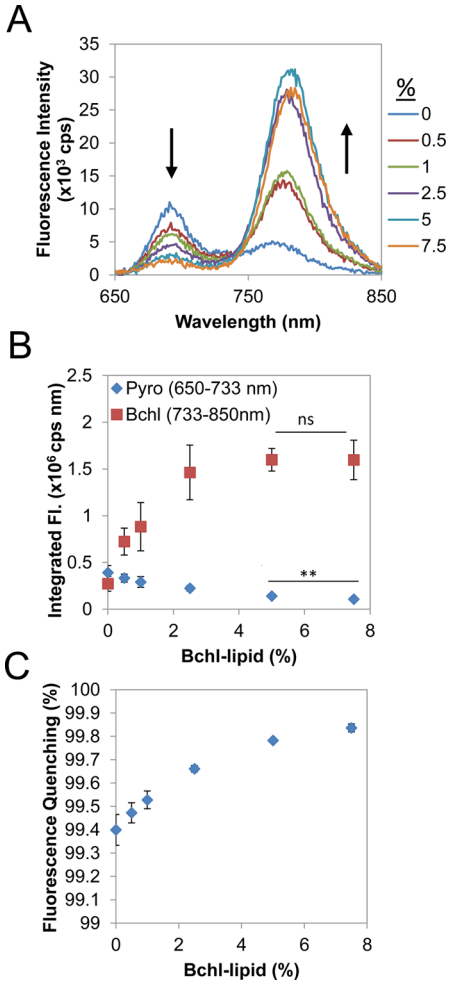

Figure 2. Fluorescence characterization of bchl-lipid doped porphysomes (A). Illustrative fluorescence spectra of bchl-lipid doped porphysomes showing the pyro-lipid emission band (650–733 nm) and bchl-lipid emission band (744–850 nm). (B) Integrated fluorescence for the pyro-lipid band (blue) and bchl-lipid band (red) as a function of bchl-lipid loading (mol/mol % of total fluorescent lipid). Each data point represents the mean ± s.d. of 3 independent samples. Two-tailed Student's *t* tests were conducted comparing the integrated fluorescence of the 5% and 7.5% samples. ** $p < 0.01$. n.s = not significant. (C) Fluorescence quenching in bchl-lipid doped porphysomes as a function of bchl-lipid loading (mol/mol % total fluorescent lipid).

concentration of bchl-lipid (1 μM) were excited with 633 nm light and the fluorescence emission arising from bchl-lipid was collected and integrated (725–850 nm) (Supporting Information Figure S3). The fluorescence emission spectra shows that the sample containing pyro-lipid increased the fluorescence of bchl-lipid over an order of magnitude higher than the comparable sample prepared in the absence of the pyro-lipid donor. We also reduced the loading of the pyro-lipid (0.28–4.12%) while maintaining bchl-lipid constant, to examine a scenario where pyro-lipid self-quenching was minimized. This was achieved by replacing pyro-lipid with the nonfluorescent 1,2-dioleoyl-*sn*-glycero-3-phosphocholine (DOPC). We found that at a fixed bchl-lipid concentration, the fluorescence emitted from this molecule increased monotonically with the loading percentage of pyro-lipid in the lipid membrane (Supporting Information Figure S4A) and culminated in a 5-fold enhancement in acceptor fluorescence at maximal pyro-lipid loading (4.12%) (Supporting Information Figure S4B). These results indicate that the observed emission originating from bchl-lipid occurs predominately as a result of energy transfer from pyro-lipid and not from direct bchl-lipid excitation.

Incorporation of an acceptor dye can affect the packing between pyro-lipid molecules which may negatively affect the photothermal properties. This in turn can alter dye quenching, which directly influences the light-to-heat conversion process. The extent of fluorescence quenching was assessed as a function of bchl-lipid loading. In the absence of bchl-lipid, pyro-lipid was found to be 99.4% quenched (Figure 2C). Pyro-lipid quenching was found to increase with increasing bchl-lipid incorporation. These quenching results suggest that the porphysome photothermal properties were not compromised by the addition of the FRET acceptor. We compared the heating capabilities of 5% FRETysomes with those of porphysomes prepared in the absence of bchl-lipid. Each sample adjusted to a concentration of 100 μM was sealed inside a quartz cuvette and irradiated for 16.7 min at 2.5 W/cm^2. At the concentration tested, both samples were able to increase the temperature of the solution beyond 50 °C, with control porphysomes displaying marginally increased photothermal heating compared to their bchl-lipid doped counterpart (Supporting Information Figure S5).

Serum Stability of Porphysomes and FRETysomes. We compared the serum stability of the two nanovesicle formulations upon incubation in fetal bovine serum (95%) over a period of 24 h. We used fluorescence unquenching as a metric to assess the stability of porphysomes. Binding and solubilization of porphyrin–lipid components are expected to lead to a decrease in fluorescence quenching efficiency. We monitored porphysome and the bchl-lipid doped FRETysome–serum interactions over a period of 24 h at 37 °C. We observed that incubation with serum led to a rapid initial decrease in fluorescence quenching (Supporting Information Figure S6). This rate decreased after 1 h at which point the quenching efficiency of porphysomes and that of FRETysome began to diverge. At 24 h, the fluorescence quenching efficiency was found to be 89% and 90% in the porphysomes and FRETysomes, respectively. These data appears to suggest that FRETysomes are slightly more serum stable than the undoped porphysomes. However, this difference in quenching efficiency only amounts to 1% over 24 h and is not expected to impact the *in vivo* performance in these two formulations.

Subcutaneous Imaging of FRETysome Fluorescence. We next assessed the ability to image FRETysomes through tissue. Porphysomes or the 5% bchl-lipid doped FRETysomes were mixed with Matrigel and injected subcutaneously into nude mice. Once the Matrigel plugs solidified, the animal was imaged by hyperspectral fluorescence imaging. Hyperspectral imaging showed fluorescence signal arising from each of the inserted plugs (Figure 3A). Fluorescence arising from the 5% FRETysomes could be clearly distinguished from porphysomes based on the signal intensity as well as the shape of the fluorescence spectrum (Figure 3B). FRETysomes displayed a fluorescence maximum at 790 nm, while porphysomes showed a broad emission spectrum with a peak centered at 730 nm. These results confirm the observations conducted *in vitro* showing that the bchl-doped version of porphysomes was more fluorescent in the intact state than the undoped porphysomes. The fact that they were successfully imaged subcutaneously indicated that this particular formulation may be suitable for

DOI: 10.1021/bc500595d
Bioconjugate Chem. 2015, 26, 345–351

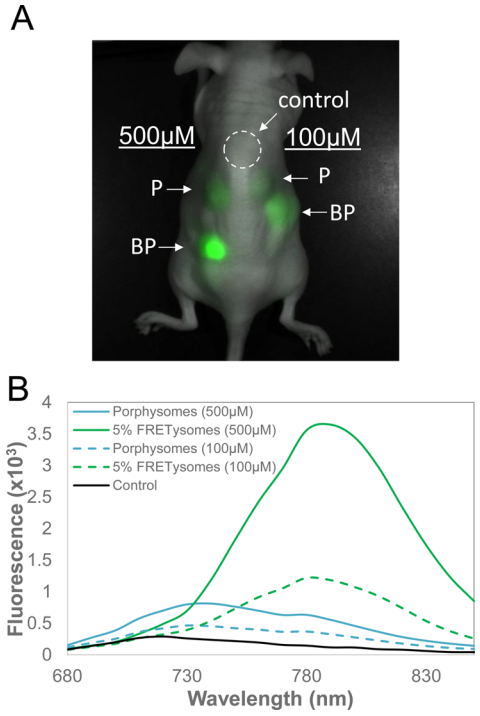

Figure 3. Subcutaneous imaging of FRETysomes. (A) Fluorescence image of animal injected with porphysomes and 5% FRETysomes embedded in Matrigel at a concentration of 100 μM or 500 μM. P, Porphysomes; BP, Bchl-lipid doped porphysomes. Dashed circle, Matrigel control. (B) Fluoresence spectra of injected samples.

fluorescently tracking the kinetics of porphysome structural degradation *in vivo*.

Kinetics of FRETysome Fluorescence in Tumor Xenografts. A KB tumor xenografts model was employed to test if the structural sensing capabilities of FRETysomes could be monitored *in vivo*. Animals were divided into two treatment groups (n = 4 in each group) and received an intravenous injection of FRETysomes (150 nmol) or porphysomes (150 nmol). Hyperspectral fluorescence images were collected over a period of 120 h. Fluorescence spectra of tumors at each time point were extracted from image cubes. Animals receiving porphysomes showed an increase in pyro-lipid emission at 720 nm over time, with maximum tumor signal occurring between 24 and 30 h postinjection (Figure 4A). These images were difficult to interpret since the increase in fluorescence from pyro-lipid could be caused by an increase in nanoparticle accumulation, as well as unquenching of pyro-lipid fluorescence which overlaps the same region. Animals injected with 5% FRETysomes showed a different evolution of fluorescence spectra over time. At early time points (<9 h), fluorescence could be observed distributed throughout the entire body. The signal originated from the FRET induced by bchl-lipid (Figure 4B). After 9 h, a decrease in FRET transfer to bchl-lipid was observed as well as an increase in pyro-lipid fluorescence. This fluorescence reached a maximum between the 24 and 30 h time points, after which fluorescence from pyro-lipid decreased due to clearance or degradation of the molecule. Image arithmetic on the grayscale images of each sample at 790 and 720 nm provided spatial information on the structural state of FRETysomes. Intact FRETysomes should have a 790 nm:720 nm ratio approaching 4, while structural degradation will cause the fluorescence ratio to decrease to a value approaching 0.25. Figure 4C shows that FRETysome signals change dynamically with time over 48 h, beginning with the distribution of the intact particle widely throughout the body in 1 h. As time passes, there appears to be an accumulation of intact particles in the tumor (24 and 48 h). There are also intact particles observed in the base of the tail as well as in the earlobe. Accumulation of intact FRETysomes in this region could be

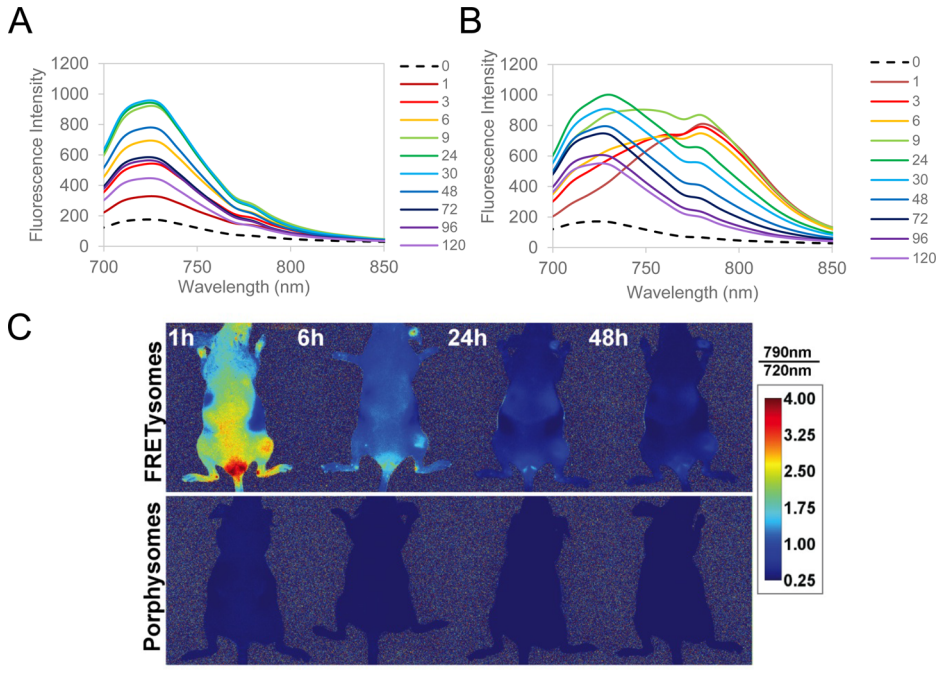

Figure 4. Ratiometric fluorescence of FRETysomes and porphysomes in KB-bearing tumor xenografts. Time evolution (in h) of fluorescence spectra in the tumors of animals injected with 150 nmol of (A) Porphysomes or (B) 5% FRETysomes. (C) Representative ratio images of fluorescence at 790 and 720 nm in FRETysome (upper panel) and porphysome (lower panel) injected animals.

DOI: 10.1021/bc500595d
Bioconjugate Chem. 2015, 26, 345−351

due to the presence of broken blood vessels which can trap FRETysomes. Beyond 6 h, a decrease in fluorescence ratio was observed indicating breakdown of the FRETysomes. In the case of animals injected with porphysomes, the fluorescence ratio measured in the tumor remained steady around 0.25 over time.

A plot of the fluorescence ratios from the tumor in FRETysome and porphysome treated groups shows that, after injection, slow disruption of the FRETysomes occurred and led to an exponential decrease in fluorescence ratios (Figure 5). This value provides information on the structural

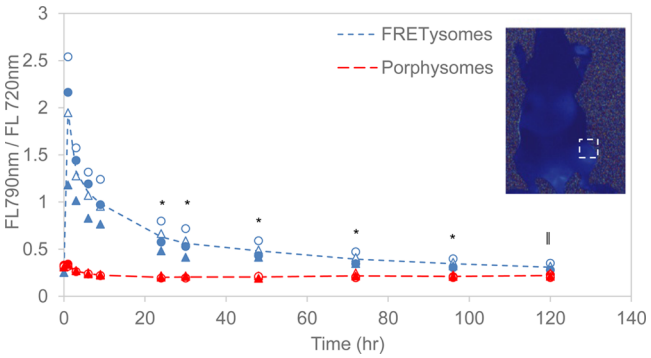

Figure 5. Plot of 790 nm:720 nm fluorescence ratio over time in animal injected with 5% FRETysomes (blue) or porphysomes (red). Data sets from each animal are represented by different symbols. The dashed lines show the mean fluorescence ratio as a function of time in each treatment group ($n = 4$ for each group). * $p < 0.001$ (two-tailed t test), ‖ $p < 0.005$ (two-tailed t test).

state of the nanoparticles. Given that disruption of the vesicles will cause a separation of the dye-pair beyond the FRET distance limit (~10 nm), structural breakdown of the porphysome was expected to cause a decrease in the fluorescence ratio. Ratios in FRETysomes were found to be greater than those in undoped porphysomes at all time points, providing evidence that intact nanovesicles remained in the tumor over the course of the entire experiment (Figure 5). More importantly, the results of these experiments also showed that between 24 and 48 h postinjection, the fluorescence ratio in the tumor was significantly higher than the fluorescence ratio expected if the particles were completely unquenched. This suggested that energy transfer between pyro-lipid and bchl-lipid was still occurring (Figure 5). Thus, structurally intact nanovesicles were still present in the tumor over this time frame and could participate in photothermal heating. This also explained the capability of porphysomes to function as a photothermal agent at 24 h, even though fluorescence unquenching was also observed over the same period of time.[3]

Solute leakage assays have typically been utilized in the investigation of liposome stability.[20−22] Because biomedical applications of liposomes revolved around their ability to retain stably encapsulate drugs and imaging agents, dye leakage was often used as the metric for determining liposome stability.[23] While the structural stability of the liposome has a direct effect on solute leakage from the aqueous core, the converse is not necessarily true. Permeability of the lipid bilayer to water and solutes can occur even while the structural morphology of the bilayer remains intact. This can be attributed to factors such as the extent of partitioning occurring in the permeant.[24] For photothermal applications of porphysomes, the packed porphyrin−lipid structure, rather than the permeability, is the key parameter for efficient light-to-heat conversion. Thus, FRET was employed as the strategy for observing bilayer stability, since separation of the lipid components will induce a change in the fluorescence spectrum, which could be monitored using hyperspectral imaging.

There are some limitations in this study which remain to be addressed. The technique presented here provided a qualitative assessment of the structural stability of porphysomes *in vivo* and was particularly useful at early time points where the comparable undoped porphysome remained fluorescently quenched. Visualization of bchl-lipid acceptor fluorescence over time provides evidence that there are still intact particles in at that location; however, this method cannot report on the concentration, nor the proportion of the structurally intact population. A quantitative assessment of concentration of particles in the structurally intact versus disrupted state would require additional information, such as that provided by another emitting label (fluorescence or radioactive) which can report the concentration of porphyrin−lipid in the tissue.

CONCLUSION

In conclusion, we demonstrated the feasibility of incorporating a fluorescence energy acceptor molecule into the vesicle structure of porphysomes. This enabled FRET between pyro-lipid to bchl-lipid while at the same time maintaining the morphological and photothermal properties of porphysomes. Energy transfer between the dye pair caused a large apparent Stokes shift of 100 nm. More importantly, by monitoring the ratio of fluorescence originating from pyro-lipid and bchl-lipid, it was possible to qualitatively assess the structural integrity of the nanovesicles. We also showed the possibility of applying this *in vivo* and provided results suggesting that FRETysomes were still intact at 24 and 48 h postinjection.

EXPERIMENTAL PROCEDURES

Materials. Pyropheophorbide-conjugated lipid (pyro-lipid) was synthesized as previously described.[1] Bacteriopheophorbide-conjugated lipid (Bchl-lipid) and DSPE PEG_{2000} was purchased from Avanti Polar Lipids. Triton X-100 was purchased from Biorad (Mississauga, ON). Matrigel was purchased from Invitrogen.

Porphysome Preparation. Porphysomes were prepared as previously described.[1] Briefly, a lipid film was prepared by combining 55 mol % of fluorophore conjugated lipid, 40% cholesterol, and 5 mol % of PEG-lipid dissolved in chloroform. The fluorophore-conjugated lipid component comprising bacteriopheophorbide−lipid ranging from 0 to 7.5 mol % of the fluorophore content with the remainder comprising pyropheophorbide−lipid. The chloroform solutions of materials were dried in a borosilicate glass tube under a stream of nitrogen gas, followed by additional drying under vacuum desiccation for at least 1 h prior to the start of the experiment. Phosphate buffered saline was added for rehydration and was then subjected to ten freeze−thaw cycles. All porphysome samples were then extruded 15 times using a manual extruder (Avanti Polar Lipids, Alabaster, AL) through a 100 nm pore size polycarbonate membrane (Whatman) at 70 °C. For large scale preparations, samples having undergone 10 freeze−thaw cycles were extruded 10 times through a 100 nm polycarbonate filter using a high-pressure extruder. Porphysome concentration was assessed by measuring the absorption in methanol, using the molar extinction coefficients of 45 000 M^{-1} cm^{-1} at 665 nm for pyro-lipid and 37 000 M^{-1} cm^{-1} at 747 nm for bchl-lipid.

DOI: 10.1021/bc500595d
Bioconjugate Chem. 2015, 26, 345−351

Porphysome *z*-average size and polydispersity were measured using a Malvern ZS90 Nanosizer (Malvern Instruments, UK). Three measures were performed with 10 runs each, and the results were averaged. Samples were stored at 4 °C until used for an experiment.

Fluorescence Characterization of FRETysomes. FRETysomes and control porphysomes were characterized by fluorescence spectroscopy after formulation. Each sample was adjusted so that the final concentration of pyro-lipid was 2 μM in PBS. Fluorescence experiments were conducted in a Fluoromax-4 fluorescence spectrophotometer (Horiba Jobin Yvon, New Jersey, NY). Samples were excited at 633 nm (excitation slit width = 5 nm) and emission was collected from 650 to 850 nm (emission slit width = 5 nm) with a 0.1 s integration time. To compare the fluorescence from each sample and to account for small shifts in wavelength between samples, fluorescence values were acquired by integrating over a range corresponding to pyro-lipid emission (acceptor; 650−733 nm) and bchl-lipid emission (733−850 nm). For fluorescence quenching experiments, samples were prepared at a concentration of 1 μM and measurements were made in PBS. After samples were measured, Triton X-100 was added such that the final concentration was 0.1% (v/v). The quenching efficiency was calculated using the following equation:

$$\%\text{quenching efficiency} = \left(1 - \frac{F_0}{F_{\text{detergent}}}\right) \times 100$$

where F_0 is the initial quenched fluorescence intensity and $F_{\text{detergent}}$ is the detergent unquenched fluorescence intensity.

The FRET efficiency was also determined for each of the samples containing bchl-lipid using the following equation:

$$\text{FRET efficiency}\,(\%) = \left(1 - \frac{F_{\text{DA}}}{F_{\text{D}}}\right) \times 100$$

where F_{DA} is fluorescence originating from the donor upon addition of acceptor (FRETysomes 0.5−5% bchl-lipid) and F_{D} corresponds to the fluorescence of the donor in the absence of the acceptor (undoped porphysomes).

Photothermal Heating Experiments. FRETysomes and porphysomes prepared at a concentration of 1.5 mM was diluted to a final concentration of 100 μM in PBS. Two milliliters of sample was transferred to a quartz cuvette loaded with a magnetic stir-bar and a thermocouple. A plastic cap was fitted over the top of the cuvette to reduce evaporation. A 660 nm laser with a fluence rate of 2.5 W/cm^2 was positioned 1 cm away from the cuvette at 1 cm above the base of the cuvette. The sample was irradiated with light while stirring and simultaneous temperature measurements were recorded. The irradiation time lasted ∼16.7 min, after which the cuvette was allowed to cool to room temperature.

Animal Experiments. All animal experiments were conducted in accordance with animal use protocols approved by University Health Network's Animal Research Committee.

Cell Culture and Tumor Inoculation. KB cells were cultured in Eagle's Minimum Essential Medium supplemented with 10% fetal bovine serum. Immediately prior to tumor inoculation, KB cells were trypsinized and washed 3 times with phosphate buffered saline. The concentration of cells was adjusted to 2 × 10^7 cells/mL and kept on ice throughout the experiment. Female nude mice (Harlan) were anaesthetized with a gaseous mixture of isofluorane and oxygen. Once induction of anesthesia was complete, the hind flank of each animal was inoculated with 2 × 10^6 KB cells.

Whole-Body Hyperspectral Fluorescence Imaging. All *in vivo* images were captured using the Maestro hyperspectral fluorescence imager (Quorum Technologies Inc., Guelph, ON) equipped with a 640 ± 25 nm excitation bandpass filter and 700 nm long-pass filter. Spectral images were acquired by scanning from 700 to 850 nm in 10 nm intervals with an exposure time of 100 ms and 2 × 2 pixel binning.

Subcutaneous Visualization of Porphysomes and FRETysomes. A female nude mouse was anaesthetized with isofluorane prior to the subcutaneous injection of porphysome or FRETysomes. Immediately, before the experiment, Matrigel (7.9 mg/mL; BD Biosciences) was mixed with 5% bchl-lipid FRETysomes, porphysomes, or saline to a final Matrigel concentration of 4 mg/mL. Mixing was done on ice to inhibit the gelation of Matrigel which occurs at physiological temperatures. Fifty microliters of sample was prepared at pyro-lipid concentrations of 100 μM or 500 μM. These samples were then injected subcutaneously using 29.5 gauge insulin syringes. Once Matrigel plugs solidified, images of the animal were acquired using the Maestro hyperspectral fluorescence imager with the FRETysome signal unmixed from the image cube.

Ratiometric Imaging of FRETysomes in Tumor Xenografts. Female nude mice (∼25 g) were inoculated with KB tumor cells. After tumors reached an average volume of 130 mm^3, animals were separated into two treatment groups designated as either the 5% bchl-lipid FRETysomes (n = 4) or porphysomes group (n = 4). All animals were imaged prior to treatment, in order to establish a baseline fluorescence signal in the tissue. Animals were injected with 150 nmol of the nanoparticle designated in their treatment group. Hyperspectral images were captured at 1, 3, 6, 9, 24, 30, 48, 72, 96, and 120 h postinjection. Regions of interest were drawn over the tumor area for each animal at each time point to record the changes in fluorescence spectrum as a function of time.

Image Processing. Ratiometric images were generated by extracting the 790 or 720 nm channels from the image cube. Images were converted to 16-bit images and image arithmetic was applied to each frame using ImageJ. The signal intensity at 790 nm was divided by the extracted image at 720 nm to generate an image of intensity ratios. These values were rescaled such that the minimum and maximum values were 0.25 and 4.0, respectively. Last, the resultant grayscale images were pseudocolored to clearly display the pixel ratios.

■ ASSOCIATED CONTENT

Supporting Information

Characterization of FRETysome formulations loaded with various amounts of bchl-lipid. (Table S1). Absorption and fluorescence spectra of pyro-lipid and bchl-lipid in methanol (Figure S1). Effect of bchl-lipid doping on porphysome absorbance spectrum (Figure S2). Comparison of fluorescence emission from FRETysomes with bchl-lipid embedded in POPC liposomes (Figure S3). Effect of reducing pyro-lipid donor (0−4.12%) loading on energy transfer in FRETysomes (Figure S4). Photothermal heating of FRETysomes and porphysomes (Figure S5). Serum stability of FRETysomes and porphysomes (Figure S6). This material is available free of charge via the Internet at http://pubs.acs.org.

DOI: 10.1021/bc500595d
Bioconjugate Chem. 2015, 26, 345−351

AUTHOR INFORMATION

Corresponding Author

*E-mail: gang.zheng@uhnres.utoronto.ca.

Notes

The authors declare no competing financial interest.

ACKNOWLEDGMENTS

This work was supported by a grant from the Natural Sciences and Engineering Research Council of Canada and the Canadian Institutes for Health Research, with additional support from the Ontario Institute for Cancer Research, Prostate Cancer Canada, the Canadian Foundation of Innovation, Princess Margaret Cancer Foundation, Terry Fox New Frontiers Program Project Grant, the Joey and Toby Tanenbaum/Brazilian Ball Chair in Prostate Cancer Research. We thank W. Chan, C. Yip, and J. Chen for insightful discussion.

REFERENCES

(1) Lovell, J. F., Jin, C. S., Huynh, E., Jin, H., Kim, C., Rubinstein, J. L., Chan, W. C., Cao, W., Wang, L. V., and Zheng, G. (2011) Porphysome nanovesicles generated by porphyrin bilayers for use as multimodal biophotonic contrast agents. *Nat. Mater. 10*, 324−32.

(2) Jin, C. S., Cui, L., Wang, F., Chen, J., and Zheng, G. (2014) Targeting-triggered porphysome nanostructure disruption for activatable photodynamic therapy. *Adv. Healthcare Mater. 3*, 1240−1249.

(3) Jin, C. S., Lovell, J. F., Chen, J., and Zheng, G. (2013) Ablation of hypoxic tumors with dose-equivalent photothermal, but not photodynamic, therapy using a nanostructured porphyrin assembly. *ACS Nano 7*, 2541−2550.

(4) Liu, T. W., MacDonald, T. D., Jin, C. S., Gold, J. M., Bristow, R. G., Wilson, B. C., and Zheng, G. (2013) Inherently multimodal nanoparticle-driven tracking and real-time delineation of orthotopic prostate tumors and micrometastases. *ACS Nano 7*, 4221−4232.

(5) MacDonald, T. D., Liu, T. W., and Zheng, G. (2014) An MRI-sensitive, non-photobleachable porphysome photothermal agent. *Angew. Chem., Int. Ed. 53*, 6956−9.

(6) Liu, T. W., MacDonald, T. D., Shi, J., Wilson, B. C., and Zheng, G. (2012) Intrinsically copper-64-labeled organic nanoparticles as radiotracers. *Angew. Chem., Int. Ed. 51*, 13128−13131.

(7) Clegg, R. M. (2006) The history of FRET: From conception through the labors of birth. *Reviews in Fluorescence* (Geddes, C., and Lakowicz, J., Eds.) pp 1−45, Springer, New York.

(8) Lakowicz, J. R. (2006) Energy transfer. *Principles of Fluorescence Spectroscopy* (Lakowicz, J. R., Ed.) pp 443−475, Springer, New York.

(9) Jares-Erijman, E. A., and Jovin, T. M. (2003) FRET Imaging. *Nat. Biotechnol. 21*, 1387−95.

(10) Truong, K., and Ikura, M. (2001) The use of FRET imaging microscopy to detect protein-protein interactions and protein conformational changes in vivo. *Curr. Opin. Struct. Biol. 11*, 573−8.

(11) Feigenson, G. W., and Buboltz, J. T. (2001) Ternary phase diagram of dipalmitoyl-pc/dilauroyl-pc/cholesterol: nanoscopic domain formation driven by cholesterol. *Biophys. J. 80*, 2775−88.

(12) Silvius, J. R. (2003) Fluorescence energy transfer reveals microdomain formation at physiological temperatures in lipid mixtures modeling the outer leaflet of the plasma membrane. *Biophys. J. 85*, 1034−45.

(13) Lovell, J. F., Chan, M. W., Qi, Q., Chen, J., and Zheng, G. (2011) Porphyrin fret acceptors for apoptosis induction and monitoring. *J. Am. Chem. Soc. 133*, 18580−18582.

(14) Wagh, A., Qian, S. Y., and Law, B. (2012) Development of biocompatible polymeric nanoparticles for in vivo nir and FRET imaging. *Bioconjugate Chem. 23*, 981−992.

(15) Lee, S.-Y., Tyler, J. Y., Kim, S., Park, K., and Cheng, J.-X. (2013) FRET imaging reveals different cellular entry routes of self-assembled and disulfide bonded polymeric micelles. *Mol. Pharmaceutics 10*, 3497−3506.

(16) Lu, J., Owen, S. C., and Shoichet, M. S. (2011) Stability of self-assembled polymeric micelles in serum. *Macromolecules 44*, 6002−6008.

(17) Lainé, A. L., Gravier, J., Henry, M., Sancey, L., Béjaud, J., Pancani, E., Wiber, M., Texier, I., Coll, J. L., Benoit, J. P., and Passirani, C. (2014) Conventional versus stealth lipid nanoparticles: formulation and in vivo fate prediction through fret monitoring. *J. Controlled Release 188*, 1−8.

(18) Zhao, Y., Schapotschnikow, P., Skajaa, T., Vlugt, T. J., Mulder, W. J., de Mello Donega, C., and Meijerink, A. (2014) Probing lipid coating dynamics of quantum dot core micelles via Forster resonance energy transfer. *Small 10*, 1163−70.

(19) Skajaa, T., Zhao, Y., van den Heuvel, D. J., Gerritsen, H. C., Cormode, D. P., Koole, R., van Schooneveld, M. M., Post, J. A., Fisher, E. A., Fayad, Z. A., de Mello Donega, C., Meijerink, A., and Mulder, W. J. (2010) Quantum dot and Cy5.5 labeled nanoparticles to investigate lipoprotein biointeractions via Forster resonance energy transfer. *Nano Lett. 10*, 5131−8.

(20) Portis, A., Newton, C., Pangborn, W., and Papahadjopoulos, D. (1979) Studies on the mechanism of membrane fusion: evidence for an intermembrane Ca^{2+}-phospholipid complex, synergism with Mg^{2+}, and inhibition by spectrin. *Biochemistry 18*, 780−90.

(21) Senior, J., and Gregoriadis, G. (1982) Stability of small unilamellar liposomes in serum and clearance from the circulation: the effect of the phospholipid and cholesterol components. *Life Sci. 30*, 2123−2136.

(22) Taira, M. C., Chiaramoni, N. S., Pecuch, K. M., and Alonso-Romanowski, S. (2004) Stability of liposomal formulations in physiological conditions for oral drug delivery. *Drug Delivery 11*, 123−128.

(23) Drummond, D. C., Meyer, O., Hong, K., Kirpotin, D. B., and Papahadjopoulos, D. (1999) Optimizing liposomes for delivery of chemotherapeutic agents to solid tumors. *Pharmacol. Rev. 51*, 691−744.

(24) Mathai, J. C., Tristram-Nagle, S., Nagle, J. F., and Zeidel, M. L. (2008) Structural determinants of water permeability through the lipid membrane. *J. Gen. Physiol. 131*, 69−76.

DOI: 10.1021/bc500595d
Bioconjugate Chem. 2015, 26, 345−351